Article

Ultrasound-Assisted Extraction of *Atractylodes chinensis* (DC.) Koidz. Polysaccharides and the Synergistic Antigastric Cancer Effect in Combination with Oxaliplatin

Minjie Liang,[§] Yayun Wu,[§] Jimin Sun, Ya Zhao, Lijuan Liu, Ruizhi Zhao,* and Yan Wang*

Read Online

ACCESS | Metrics & More | Article Recommendations

ABSTRACT: Oxaliplatin (OXA) is recognized as a first-line drug for gastric cancer. However, low accumulation of the OXA in the target site and the development of drug resistance directly led to treatment failure. In the present study, an ultrasonic extraction method for *Atractylodes chinensis* (DC.) Koidz. polysaccharides (AKUs) and the combination treatment with OXA in vitro were studied. Results showed that when the pH level was 11, the ultrasound power at 450 W, the solid−liquid ratio was 1:20, and the ultrasound treatment for 30 min, the yield of AKUs was significantly increased to 13.20 ± 0.35%. The molecular weights of the AKUs ranged from 7.21 to 185.94 kDa, and its monosaccharides were mainly composed of arabinose (Ara), galactose (Gal), and glucose (Glu) with a ratio of 58.36, 16.90, and 15.49%, respectively. Cell experiments showed that, compared to OXA alone (2 μg/mL, inhibition rate of 18%), the treatment of OXA with AKUs had a significant synergistic inhibitory effect on MKN45 proliferation, which increased to 33, 41, and 45% with increasing AKUs concentrations (5−50 μg/mL), respectively, representing a 2.5-fold inhibition. Inductively coupled plasma-mass spectrometry (ICP-MS) determination confirmed that AKUs significantly increased the intracellular uptake of OXA by 29%, compared to that of OXA alone. We first demonstrated that the combined synergistic inhibitory effect of AKUs and OXA on gastric cancer cells was mediated by reducing the expression of efflux proteins (MRP1 and MRP2) and increasing the expression of ingested protein (OCT2). As a result of the above, AKUs deserved to be an effective adjuvant combined with chemotherapeutics in a clinical setting.
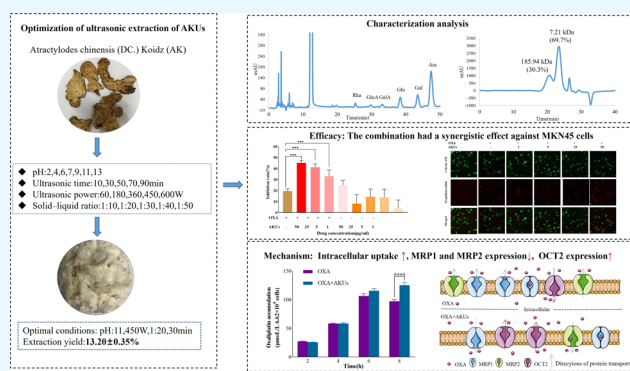
1. INTRODUCTION

According to the latest epidemiological data in 2023,[1] gastric cancer is one of the most prevalent malignant tumors worldwide, ranking fifth in incidence and fourth in mortality among all malignancies; it has a profound impact on the lives of individuals. Due to the atypical symptoms of early-stage gastric cancer, patients are often diagnosed at an advanced stage.[2] Chemotherapy is still one of the most important treatment methods for patients with advanced gastric cancer.[3,4] Oxaliplatin and other drugs can effectively kill cancer cells and prolong the survival time of patients, which are the first-line drugs for the treatment of gastric cancer.[5,6] Although oxaliplatin has shown the advantages of definite efficacy in clinical practice, it still has the problem of drug resistance by reducing the effective concentration in cells through two pathways: reducing drugs into cancer cells or increasing efflux.[7,8] MRP1 and MRP2 are one of the main membrane proteins that transport oxaliplatin and are related to the occurrence of platinum drug resistance.[9,10] Combination therapy can enhance the efficacy of chemotherapeutic agents, reduce the dosage, minimize side effects, and even overcome tumor resistance,[11,12] but suitable combination drugs are lacking. Therefore, administration of multidrug resistance reversal agents or chemotherapy sensitizers is an effective means to solve this problem.[13−15]

Recently, polysaccharides obtained from natural herbals have received increasing attention due to their remarkable biological activities and unique physicochemical properties.[16,17] More and more reports have shown that these bioactive macromolecules exhibit a variety of systemic pharmacological activities, including antitumor, immune regulation, and liver protection.[14,18] *Atractylodes chinensis* (DC.) Koidz. (AK) is a medicinal herb that plays an important role in maintaining human health and treating diseases.[19,20] *A. chinensis* (DC.) Koidz. polysaccharides (AKUs) are one of the
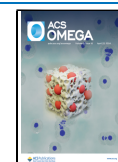
effective components of AK, which has antitumor, antiradiation, antioxidation, anti-inflammation, hypoglycemic, liver protection, and immune regulation effects.[21,22] Previous laboratory studies[23] found that ultrasound-assisted extraction of *A. chinensis* (DC.) Koidz. polysaccharides (AKPs) had a synergistic effect in combination with apatinib against gastric carcinoma to some extent, but its yield rate was lower, and the synergistic mechanism remains unclear. Therefore, we first aim to improve the yield of AKUs and then deeply study the synergistic effect and mechanism of the combined treatment of AKUs and OXA on MKN45 cell proliferation.

2. MATERIALS AND METHODS

2.1. Materials and Reagents. The roots of *A. chinensis* (DC.) Koidz. (210301) were purchased from Guangzhou Zisun Pharmaceutical Co., Ltd. (Guangzhou, China) and authenticated by Nengfeng Ou, the pharmacist in charge of assessing herb quality at the Second Affiliated Hospital of Guangzhou University of Chinese Medicine. MKN45 cells were purchased from the China Center for Type Culture Collection (Wuhan, China). Oxaliplatin (20220223) was purchased from Jiangsu Hengrui Pharmaceutical Co., Ltd. (Chengdu, China). RIPA lysis buffer (P0013B) was purchased from Beyotime Biotechnology Co., Ltd. (Shanghai China). The monosaccharide standards were purchased from Yuanye Biotechnology Co., Ltd. (Shanghai, China). Dextran standards were purchased from the American Polymers Standards Corporation (USA). Antibodies against OCT2 (ab179808), MRP1 (ab260038), and MRP2 (ab15603) were purchased from Abcam (Cambridge, UK). GAPDH (D16H11, CST, Danvers, MA) and Pt ICP-MS standard solution (060078-04-01) were purchased from O2si Smart Solutions (North Charleston, USA).

2.2. Extraction of Polysaccharides. The raw materials were crushed by using a grinder and passed through a five-mesh sieve. Before ultrasound extraction, the powder was degreased twice with 70% ethanol and subsequently dried.[24] The ultrasound-assisted extraction and single-factor extraction experiments were conducted according to previously described methods with slight modifications.[25] Briefly, 20 g of degreased product was first extracted by ultrasonication and filtered. Then, the products were alcohol precipitated overnight, dialyzed against a 3000 Da dialysis bag for 72 h, and freeze-dried (Labconco FreeZone6, Labconco Co., Kansas City, MO, USA) to obtain polysaccharides.

The ultrasound extraction process is influenced by factors such as the solvent pH, ultrasound power, time, and solid–liquid ratio.[25] Therefore, in this study, we compared the four key parameters. The ultrasound extraction single-factor experiment was designed as follows. The solvent pH was maintained at 2, 4, 6, 7, 9, 11, or 13 (adjusting with glacial acetic acid or ammonia–water). The obtained optimal single factor was used as a fixed condition for the single-factor experiments. The extraction was performed at 10, 30, 50, 70, and 90 min. The solid–liquid ratio was maintained at 1:10, 1:20, 1:30, 1:40, and 1:50 g/mL, and the power was maintained at 60, 180, 300, 450, and 600 W. The extraction yield of polysaccharides was calculated using eq 1.

$$\text{Polysaccharide yield } (\%, \text{ w/w})$$
$$= \frac{\text{weight of dried AKUs (g)}}{\text{weight of pretreated AKUs powder a (g)}} \times 100$$
(1)

2.3. Characteristics of AKUs. *2.3.1. Spectroscopic Analysis.* Three mg of AKUs was prepared into 1 mg/mL polysaccharide solution with distilled water. The solution was analyzed using a U-2910 ultraviolet spectrophotometer in the range of 600−200 nm. Two mg of AKUs was taken and scanned in the range of 400−4000 cm^{-1} on an FT-IR spectrophotometer (Spectrum Two, PerkinElmer, Waltham, MA, USA).

2.3.2. Structural Information Analysis. The molecular weight was determined by HPLC (Agilent 1260, Santa Clara, CA, USA) equipped with a refractive index detector (RID) and a TSKgel GMPWXL column (7.8 × 300 mm; Tosoh Corporation, Yamaguchi, Japan). The temperature of the column chamber was set at 30 °C, the sample was eluted with 0.2 M NaCl at a flow rate of 0.4 mL/min.[18] The calibration curves of glucans with different molecular weights (M_w) (1, 4, 95, 820, 950, and 3755 kDa) were obtained for calculating the molecular weight.

The monosaccharide content in the AKUs was determined by complete acid hydrolysis combined with PMP precolumn derivatization.[26] In short, 5 mg of dried AKUs was hydrolyzed with 4 mL of trifluoroacetic acid (TFA, 4 M) at 110 °C for 4 h under a nitrogen atmosphere. After that, the sample was mixed with equal volume 0.6 mol/L 1-phenyl-3-methyl-5-pyrazolone (PMP) and 0.3 mol/L NaOH solution and incubated at 70 °C for 100 min. After cooling, 0.3 mol/L HCl solution was used for neutralization and chloroform was added for extraction. The sample solutions were analyzed by Agilent 1260 HPLC (Agilent Technologies, Santa Clara, CA, USA) with a diode array detector (DAD) at a wavelength of 254 nm and with a Diamonsil C18 column (250 × 4.6 mm, 5 μm Dikema Technology Co., Ltd., Beijing, China). The mobile phase for elution was 0.05 mol/L phosphate buffer (Na_2HPO_4−NaH_2PO_4, pH = 6.83) plus acetonitrile (83:17, v/v).

2.3.3. Size and Charge Analysis. The particle size distribution and zeta potential of the AKUs solution (1 mg/mL) were measured using a NanoBrook 90 Plus PALS instrument (Brookhaven Instruments, Holtsville, NY, USA) and analyzed by Particle Solutions v.3.6.07122 (Holtsville, NY, USA).

2.4. Determining In Vitro Synergistic Activity. *2.4.1. Cell Culture.* MKN45 cells were cultured in RPMI-1640 medium supplemented with 10% FBS and 1% Pen & Strep in an incubator at 37 °C with 5% CO_2. Cells were collected in the exponential growth phase to study the antitumor effect.

2.4.2. Cell Proliferation Assay. The inhibitory effects of AKUs and OXA on MKN45 cell viability were determined by MTT assay. MKN45 cells were seeded in 96-well plates at an initial density of 3×10^3 cells/well. The cells were cultured for 24 h and then treated with OXA, AKUs, or OXA + AKUs at different predetermined concentrations. After 48 h, 20 μL of MTT (5 mg/mL) was added to each well, and the wells were incubated for another 4 h. The supernatants were removed, and 150 μL of dimethyl sulfoxide (DMSO) was added. The absorbance was measured at 490 nm by using a microplate reader (Infinite M1000Pro, Tecan, Switzerland). The combi-

nation index was expressed in terms of the Q value,[27] which was calculated using eq 2. Synergism: $Q > 1.15$; additive effect: $Q = 0.85-1.15$; antagonistic effect: $Q < 0.85$.

$$Q = R(A + B)\frac{R(A + B)}{(RA + RB - RA \times RB)} \quad (2)$$

2.4.3. Staining of Live/Dead Cells. MKN45 cells were seeded in 6-well plates (1×10^5 cells per well) for 24 h. After 48 h, the MKN45 cells were collected and stained using a live/dead staining kit. Finally, the live-/dead-stained cells were observed under a microscope (ECLIPSE Ti2-E, Nikon).

2.4.4. Cellular Uptake. First, 1×10^6 MKN45 cells were seeded in culture dishes and incubated for 24 h. Then, the cells were treated with OXA alone (20 μg/mL) or AKUs (50 μg/mL) + OXA (20 μg/mL) for 2, 4, 6, or 8 h. Cells were digested with trypsin and resuspended in PBS for counting. The suspension was centrifuged to obtain cell precipitates. Finally, it was treated with nitric acid using a microwave digester according to the procedure described in Table 1. The OXA

Table 1. Digestion Program Used To Digest Cells

temperature climb time (t/min)	temperature (T/°C)	maintaining time (t/min)	power (P/W)
10	120	3	1000
5	150	5	1000
5	190	20	1000

concentration in the cells was quantified based on the presence of platinum ions, which was determined via inductively coupled plasma-mass spectrometry (ICP-MS) (model number: 8800ICP-MS, Agilent Company, USA). The ICP-MS conditions are described in Table 2. The Pt standard was diluted

Table 2. Optimal ICP-MS Operating Parameters

parameters	value
RF power (W)	1550
sample depth (mm)	8.00
plasma gas (mL/min)	15
helium flow (mL/min)	5
atomizing chamber temperature (°C)	2
peristaltic pump (rps)	0.5
eight-stage rod RF (V)	150
energy discrimination (V)	5.0
Omega deflection voltage (V)	−110
Omega lens voltage (V)	9.6

with 2% nitric acid to produce solutions with concentrations of 0.98, 1.95, 3.9 7.8, 15.6, 31.25,62.5, 125, and 250 μg/L. The QC samples were prepared by adding blank cells at concentrations of 1.95, 7.8, and 31.625 μg/L. The method included determining the recovery and intraday and interday precision. Six replicates were analyzed, and the data are expressed as the relative standard deviation (RSD). The OXA concentration was calculated using eq 3, where 397.29 was the relative molecular weight of the oxaliplatin mixture and 195.08 was the relative molecular weight of the platinum mixture.

$$\text{Oxaliplatin content} = \frac{\text{Platinum content detected} \times 397.29}{195.08} \quad (3)$$

2.4.5. Western Blotting Analysis. The cells were cultured as described in Section 2.4.4. The cells were collected after treatment for 8 h. Total protein was extracted using RIPA lysis buffer containing 1% PMSF. The proteins were quantified using a BCA protein assay kit with BSA serving as the standard. A mixture of 10 μL of protein and 5× loading buffer was boiled at 100 °C for 5 min and loaded on a spacer gel (double distilled water, 30% acrylamide, 1.5 mol/L Tris (pH 6.8), 10% SDS, 10% ammonium persulfate, TEMED). Then, the proteins were separated on an 8% SDS−PAGE gel (double distilled water, 30% acrylamide, 1.5 mol/L Tris [pH 8.8], 10% SDS, and 10% ammonium persulfate [TEMED]). The separated proteins were transferred onto PVDF membranes (TRANS-BLOT SD SEMI DRY TRANSFER cells) with a semidry transfer solution. The membrane was partially blocked for 2 h in TBST buffer containing 5% BSA and incubated overnight at 4 °C with different primary antibodies (against MRP1, MRP2, OCT2, and GAPDH). The membranes were washed with TBST and incubated with HRP-conjugated goat antirabbit secondary antibodies for 2 h. Afterward, the membranes were washed again and subsequently analyzed using an enhanced chemiluminescence (ECL) system after exposure to X-ray films.

2.5. Statistical Analysis. The data were expressed as the mean ± standard deviation (SD). Origin 2021 (Origin Lab Corporation, Northampton, NC, USA) and GraphPad Prism 8.0 (GraphPad Software, Inc., San Diego, CA, USA) were used for analyzing the data and plotting the graphs. The differences among groups were evaluated by one-way ANOVA and Tukey's test (using GraphPad Prism 8.0). All differences between groups were considered to be statistically significant at $p < 0.05$.

3. RESULTS AND DISCUSSION

3.1. Effect of Different Factors on the Efficiency of Ultrasound-Assisted Extraction. The yield of polysaccharides is an important factor affecting drug development. Therefore, we compared the effects of the solvent, pH, ultrasonication time, ultrasonication power, and solid−liquid ratio on the efficacy of ultrasonic extraction of AKUs. The results showed that alkaline solvents extracted more AKUs than did acidic solvents (Figure 1A). When the pH was 13, the yield of AKUs was 9.58 ± 0.18%. However, because a large quantity of ammonia−water was used at pH 13, a large quantity of acetic acid was required for neutralization, which resulted in salt crystallization and the precipitation of a large number of pigments. The extraction process was complicated and expensive, and the yield at pH 13 was similar to that at pH 11. Our results indicated that, compared to ultrasonic acid extraction and ultrasonic water extraction, ultrasonic alkali extraction had the highest extraction rate. The follow-up single-factor experimental operation was conducted at pH 11.

The ultrasonication time is a key parameter affecting the yield of AKUs.[28] The yield of AKUs increased rapidly as the extraction time increased and reached an extreme value of 12.40 ± 0.37% at 30 min (Figure 1B). When the extraction time was prolonged, the increase in thermal activity accelerated the outflow of polysaccharides from the raw materials, whereas the polysaccharides in the solution were degraded due to the time accumulation effect; thus, the yield of polysaccharides decreased.

The ultrasound power is a key parameter affecting the extraction rate and activity of polysaccharides, especially at the
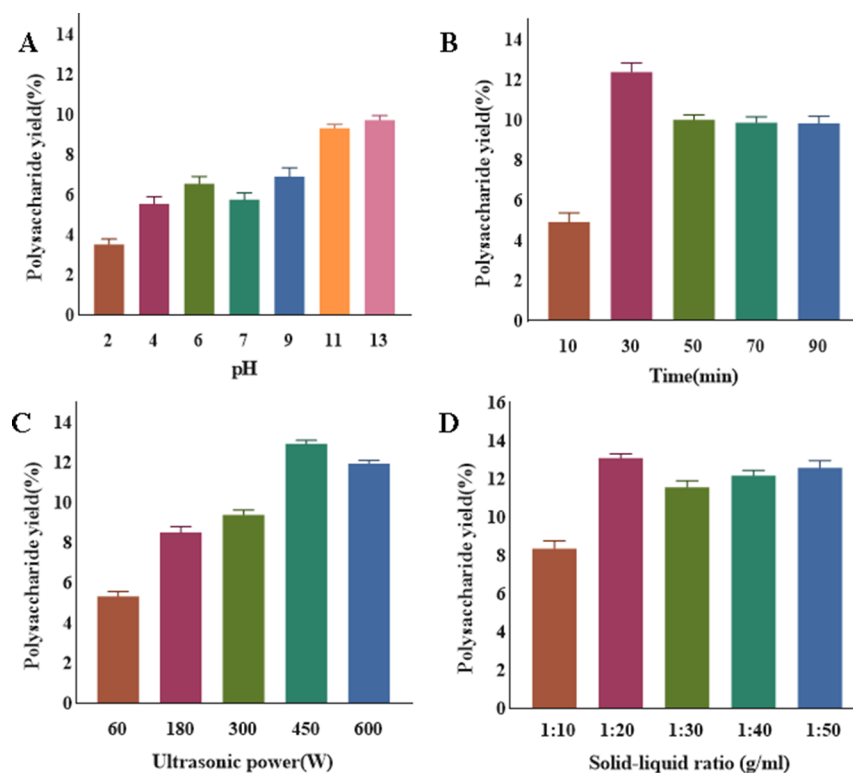
Figure 1. Effects of different factors on the extraction rate of polysaccharides. The effect of solvent pH (A), ultrasonic power (B), ultrasonication time (C), and the solid−liquid ratio (D) on the yield of AKUs.

industrial scale. As the power increased, the yield of the AKUs first increased significantly and then decreased gradually (Figure 1C). The highest yield was 12.93 ± 0.15% when the power was 450 W. Ultrasonication in this range of power generates large cavitation bubbles, which implode violently, causing cell degradation and enhancing solvent penetration.[29]

Determining the optimum amount of solvent to be used is important not only for enhancing the extraction yield and efficiency but also from an economic perspective.[30] The yield of AKUs increased faster with an increasing solid−liquid ratio (Figure 1D). This difference likely occurred because of an increase in the solid−liquid ratio, which resulted in increased osmotic pressure in the cells and accelerated the efflux of intracellular material.[31] The rapid increase in yield continued until the solid−liquid ratio reached 20 mL/mg, at which point the yield of AKUs also reached the highest value of 13.10 ± 0.19%.

Based on the experimental results for pH, ultrasonication time, ultrasonication power, and solid−liquid ratio, the optimal conditions for the ultrasound-assisted extraction of AKUs were as follows: pH 11, solid−liquid ratio: 1:20, ultrasonic power: 450 W, and ultrasonication time: 30 min. Under these conditions, the polysaccharide extraction yield was 13.20 ± 0.35%, which was almost four times the yield recorded in our previous study.

3.2. Characterization of AKUs.
3.2.1. Spectroscopic Analysis. Absorption peaks at 260 and 280 nm indicated the presence of nucleic acid conjugates and proteins.[32] The UV−vis profiles of the AKUs are shown in Figure 2A. No prominent peak corresponding to AKUs was found, which suggested that nucleic acids and proteins were present in trace amounts. These findings agreed with the recorded protein content of 2.72%.

The infrared spectrum of AKUs was shown in Figure 2B. A wide peak at 3293 cm^{-1} indicated a sugar O−H tensile vibration. The peak at 2935 cm^{-1} probably corresponded to the stretching and symmetric deformation vibrations of C−H. The absorption peaks at 1607 and 1413 cm^{-1} were attributed to symmetric vibrations of carboxyl groups.[33] The absorption peak in the range of 1475−1300 cm^{-1} represented the vibration of C−H and the deformation of methyl groups, and the absorption peak in the range of 1200−1000 cm^{-1} represented the stretching vibration of C−OH or C−O−C.[11] The characteristic absorption at 990 cm^{-1} was attributed to the symmetric stretching vibration of the furan ring, which suggested that AKUs can exist as furanose.

3.2.2. Molecular Weights of AKUs. The logarithm of the molecular weight ($\log(M_w)$) is linearly related to the retention time (T) of the polymers in the gel permeation chromatogram. By plotting the $\log M_w$ of the dextran standard on the x-axis and the retention time (T) on the y-axis, we obtained a standard curve of relative $\log M_w$. The average $\log M_w$ distribution of AKUs included two main fractions, fraction I and fraction II (Figure 2C). Fraction I corresponded to the peak of polysaccharides with a high molecular weight (185.94 kDa) and accounted for 30.3%. Fraction II corresponded to the peak of polysaccharides with a low molecular weight (7.21 kDa), accounting for 69.7%.

3.2.3. Monosaccharide Composition of AKUs. The monosaccharides of the AKUs were identified by comparing their retention times with those of the standards (Figure 2D,E). The proportion of each monosaccharide in the AKUs was calculated according to the standard equation and molar mass. The results showed that the monosaccharides of the AKUs were mainly composed of Ara, Gal, Glu, Rha, GalA, and GluA, with a molar ratio of 58.36:16.90:15.49:3.72:3.45:2.08.
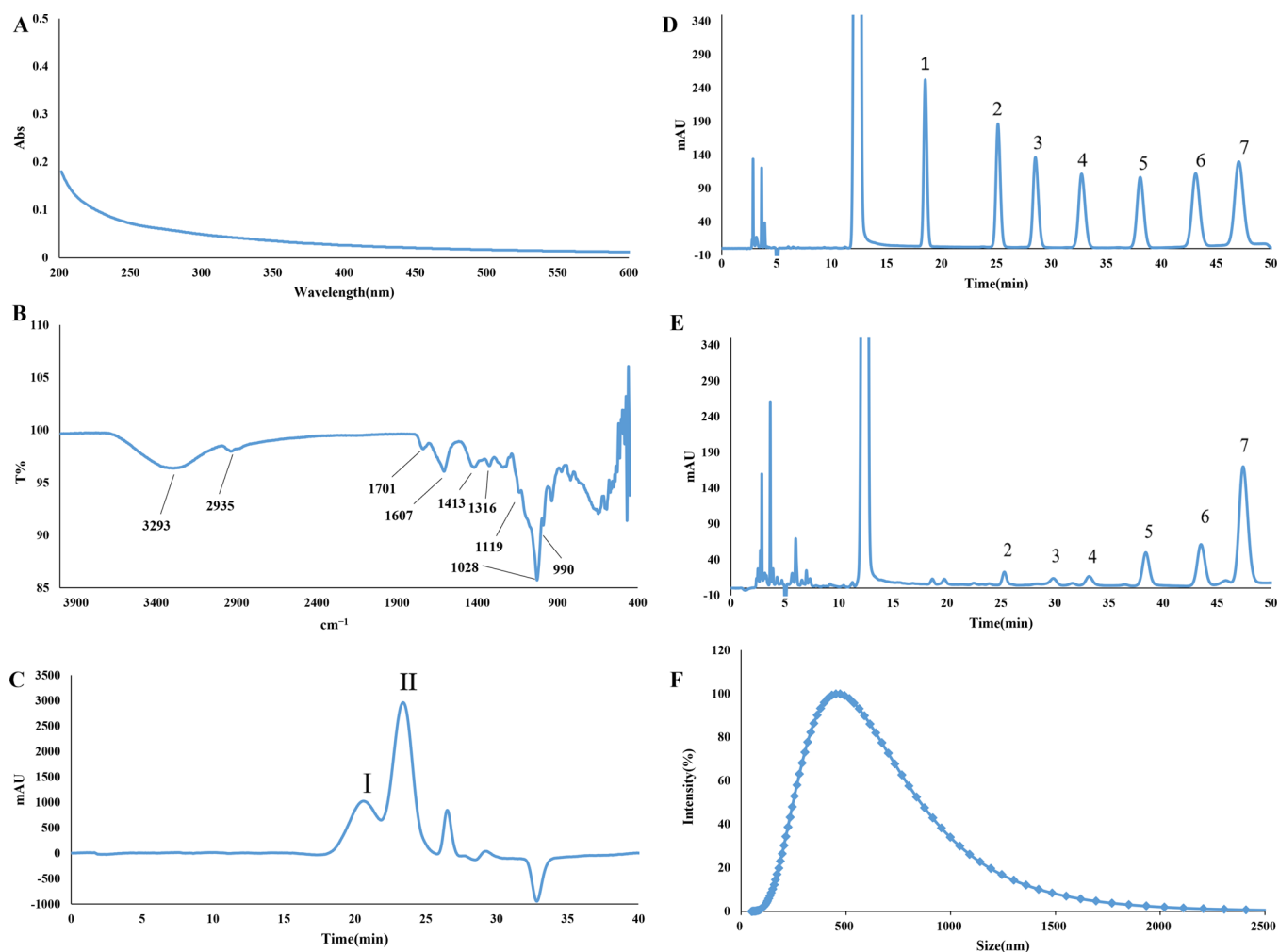
Figure 2. Characterization of the AKUs. (A) Ultraviolet scanning spectrum of the AKUs (600−200 nm). (B) Infrared spectroscopy of the AKUs. (C) HPGPC chromatogram of the AKUs. (D) HPLC spectrum of the monosaccharide composition standard (1: Man; 2: Rha; 3: GluA; 4: GalA; 5: Glu; 6: Gal; 7: Ara). (E) HPLC profile of the monosaccharide composition of the AKUs. (F) Intensity-weighted size distributions of the AKUs in water.

3.2.4. Particle Size and Potential Analysis. The particle size of the AKUs was mainly distributed between 609 and 723 nm (Figure 2F), accounting for 68.83% of the total particle size. The average zeta potential of the AKUs was −38.54 ± 0.20 mV.

3.3. In Vitro Synergistic Activity Study. *3.3.1. AKUs Promoted OXA-Induced Cell Proliferation.* We found that AKUs significantly enhanced the antigastric cancer effect of OXA in a dose-dependent manner (Figure 3A,B). After 48 h of administration, the MTT assay showed that compared to treatment with OXA alone (2 µg/mL; inhibition rate of 18%), treatment with AKUs combined with OXA had a significant synergistic effect on gastric cancer MKN45 cells. The effect became more pronounced with increasing AKUs concentration (5−50 µg/mL). The inhibition rates were 33, 41, and 45%, and the combined indices were 1.16, 1.40, and 1.72 (Q > 1.15), respectively. When the AKUs concentration was 50 µg/ mL, the OXA concentration was 2 µg/mL, and the combination had an obvious synergistic effect; thus, these agents were chosen for follow-up experiments.

3.3.2. Cell Life/Death Staining. To confirm that the combination of AKUs and OXA had synergistic effects on MKN45 cells, we performed live/dead cell staining experi-

ments. As the concentration of AKUs increased, the intensity of red fluorescence (dead cells) increased, and the intensity of green fluorescence (living cells) decreased (Figure 3C). Combined treatment with AKUs (50 µg/mL) and OXA (2 µg/mL) increased the number of dead cells, induced sustained apoptosis in MKN45 cells, and significantly decreased the cell viability. These results were similar to those of the MTT experiment, which further indicated that the combined administration of AKUs and OXA had a synergistic effect.

3.3.3. AKUs Promoted OXA Cellular Uptake. Method validation showed that there was no endogenous interference compared with the blank cell solution, which met the specificity requirement (Figure 4A−C). The Pt^{195} standard curve obtained by the external standard method is shown in Figure 4D, and the equation corresponding to the curve was $y = 33521x + 30375$ ($R^2 = 0.9999$, 0.98−250 ng/mL). The curve showed good linearity and was suitable for calculating the content. The recoveries of the low, middle, and high doses were 109.59, 106.07, and 97.89%, respectively. The intraday RSDs were 3.50, 2.45, and 4.86%, and the interday RSDs were 4.60, 2.73, and 2.42%, respectively. The recoveries and precision of this experiment met the requirements of an in vivo analysis.
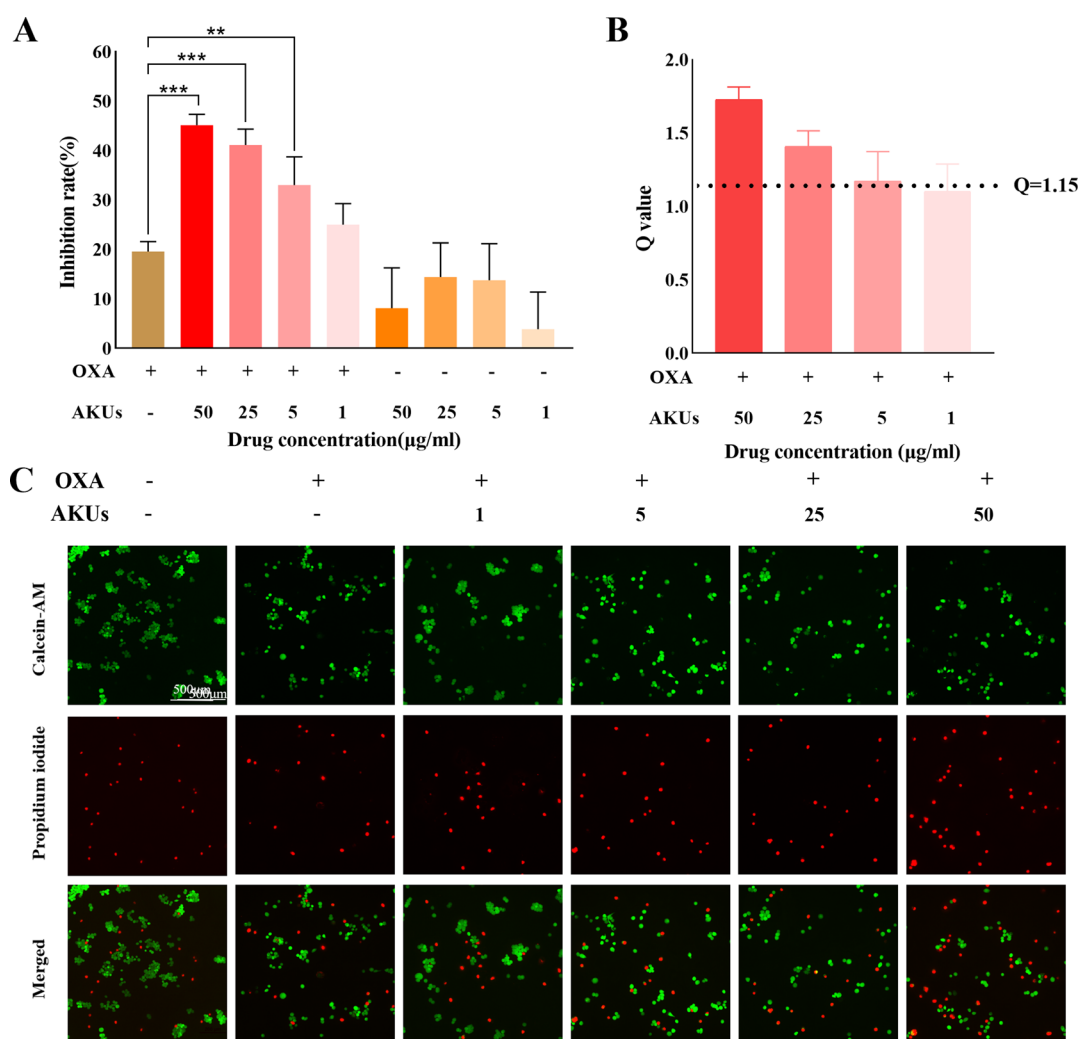
Figure 3. Effect of AKUs on the antiproliferative activity of OXA (2 μg/mL) against MKN45 cells. (A) Inhibitory effect. (B) Q value. (C) Live/dead staining images of MKN45 cells after various treatments; green indicates live cells, and red indicates dead cells. Note that "**$p < 0.01$, and ***$p < 0.001$" represent significant differences compared to the OXA group.

The uptake of the OXA by MKN45 cells was measured after 2, 4, 6, and 8 h, and the results showed that the intracellular concentration and effect of AKUs increased with time (Figure 4E). After 8 h of treatment, AKUs (50 μg/mL) significantly increased the relative cellular uptake rate of OXA from 97.34 to 125.31 μmol/L (6.62×10^5 cells) ($P < 0.001$), indicating an increase of 29%.

3.3.4. Expression of Transporters. Drug transporters are the key factors that affect drug distribution.[34,35] Therefore, we measured the influx and efflux of transporter proteins in this study. Our results showed that OXA upregulated the expression of MRP1 and MRP2 in MKN45 cells compared to their expression in the cells of the control group, these results were similar to clinical findings. Compared to OXA monotherapy, combination therapy with OXA and AKUs significantly downregulated the expression of MRP1 and MRP2 in MKN45 cells by 48.31% ($P < 0.05$) and 27.24% ($P < 0.05$), respectively (Figure 5A−C). Compared to OXA monotherapy, AKUs combination therapy significantly upregulated the expression of OCT2 in MKN45 cells by 65.7% ($P < 0.05$) (Figure 5A,D). These results indicated that the combination of AKUs and OXA inhibited the expression of the efflux transporters MRP1 and MRP2 in cells and promoted the expression of influx transporter OCT2.

4. DISCUSSION

Our previous work[24] showed that polysaccharides from AK by ultrasonic extraction (ultrasonic power 150 W, 60 °C, 40 min) had a synergistic effect when combined with apatinib, but the yield of AKPs was only 3.2%. By analyzing the mechanism of the ultrasound extraction process, the high temperature and high pressure produced by ultrasonic cavitation can lead to the destruction of the cell wall and enhance the penetration of the solvent. At the same time, the rapid formation and collapse of air bubbles can lead to changes in the structure and activity of polysaccharides.[36] All of these factors can affect the yield and physicochemical properties of polysaccharides. Therefore, some main factors are strongly needed to be optimized for higher yield without destroying the structure. Encouragingly, in this experiment, the yield of AKUs was increased to 13.20 ± 0.35% under a condition that the extraction solvent pH value was 11, ultrasonic power at 450 W, ultrasonic time for 30 min, and the solid−liquid ratio at 1:20. Arabinose, galactose, and glucose were the major part of AKPs, and there was no more change in AKUs. Interestingly, the proportion of acid sugar
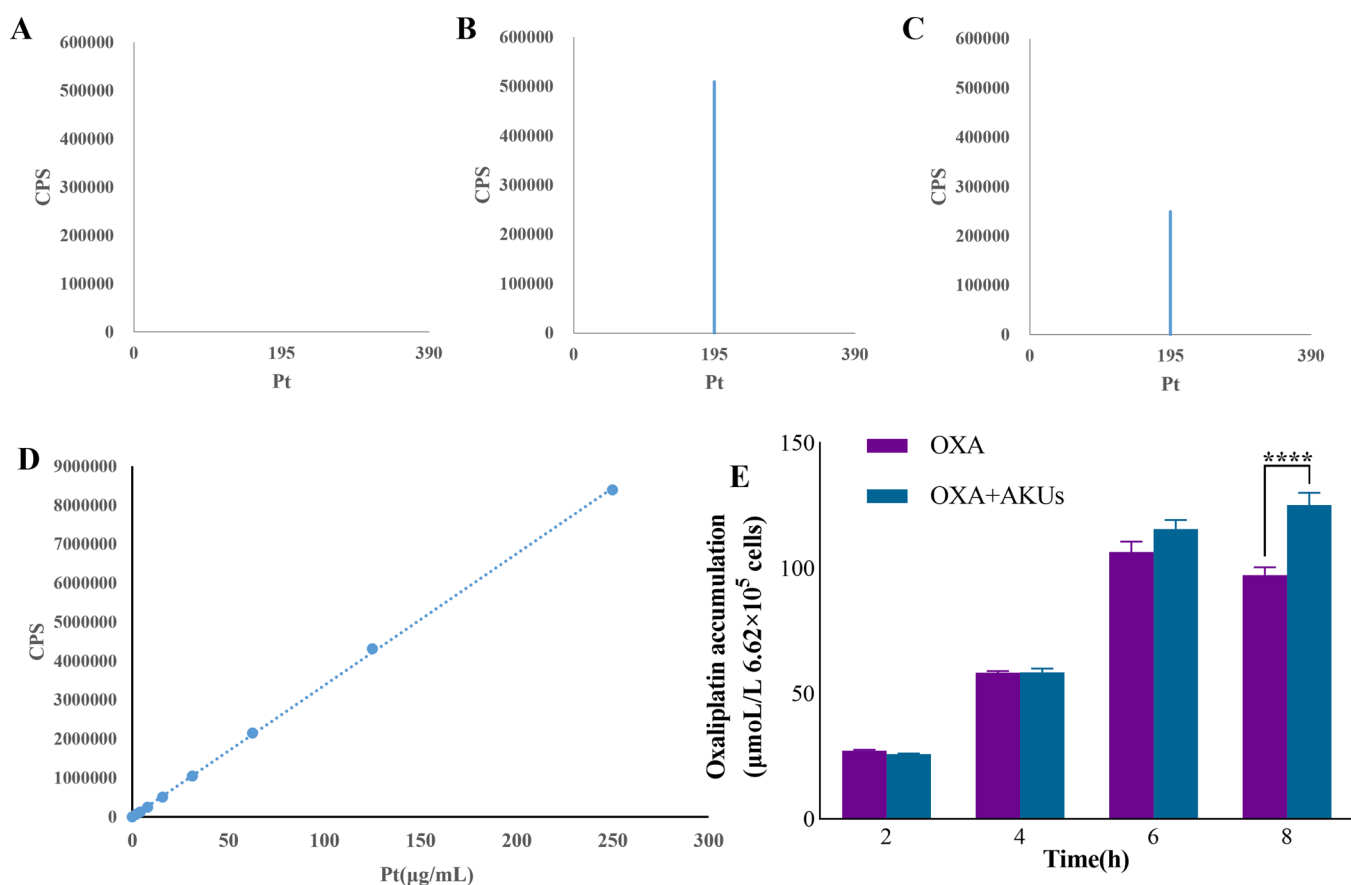
Figure 4. Effect of AKUs on OXA uptake in MKN45 cells. (A) Pt[195] concentration in a blank cell. (B) Pt[195] concentration in blank cells + OXA. (C) Pt[195] concentration in AKUs (50 μg/mL) + OXA (20 μg/mL). (D) Standard curve of Pt[195]. (E) Uptake of OXA in MKN45 cells under different treatment conditions is presented. Note that "****$p < 0.0001$" represent significant differences compared to the OXA group.
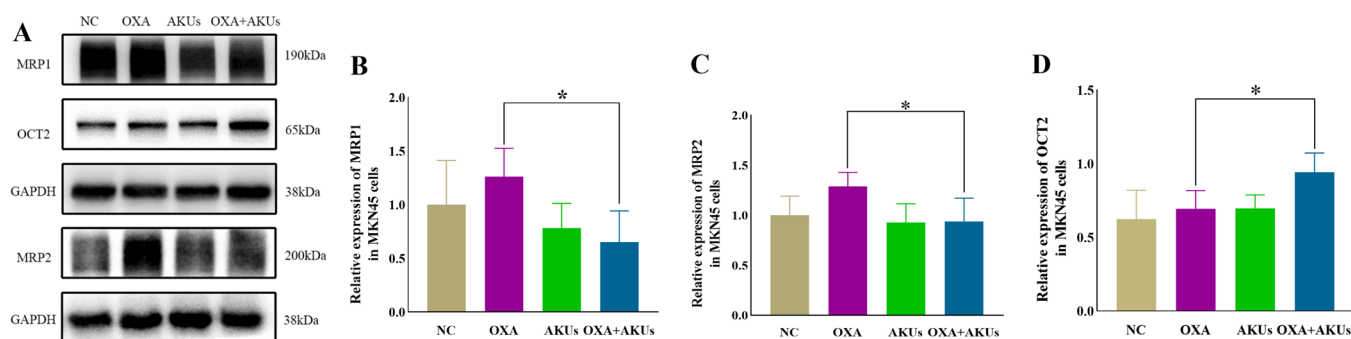
Figure 5. Effect of AKUs combined with OXA on transporters expression of MKN45 cells. (A) Proteins blots of MRP1, MRP2 and OCT2 in MKN45 cells, (B) Relative expression of MRP1 in MKN45 cells, (C) Relative expression of MRP2 in MKN45 cells, (D) Relative expression of OCT2 in MKN45 cells. Note that "*p" < 0.05 represent significant differences compared to the OXA group.

and rhamnose was increased, which was closely related to biological activity.[37] In previous reports, AKPs combined with apatinib had the antigastric cancer effect. Apatinib is an antiangiogenesis inhibitor, which can inhibit the formation of tumor neovascularization by binding to and inhibiting vascular cell growth factor receptor-2 so as to control tumor growth and become a third-line chemotherapy drug for gastric cancer.[38] Compared with apatinib, Oxaliplatin (OXA) is a third-generation platinum-based anticancer drug containing diaminocyclohexane, which plays a DNA-targeted anticancer effect by inhibiting DNA replication and arresting the cell cycle in G_0/G_1 phase.[39] It is currently the first-line chemotherapy drug for gastric cancer in clinical practice,[6] and it is cheaper and

more applicable for most populations. Current results showed that AKUs had a synergistic effect both on molecular targeted drugs and platinum anticancer drugs, suggesting that AKUs have the potential to be a sensitizer for a synergistic anticancer effect.

As we all know, chemotherapy is characterized by high lethality, which can kill cells in normal tissues while killing cancer cells, destroying the human immune system, and leading to complications such as infection after chemotherapy. Therefore, it is significant to concentrate the drug on cancer cells rather than on the normal site.[40] A recent review pointed out that the effective rate of conventional chemotherapy is less than 10%. The results showed that AKUs significantly

increased the intracellular concentration of oxaliplatin by 29%, indicating the significance of AKUs in increasing the level of intracellular accumulation of oxaliplatin. In the same time, it is meaningful that an ICP-MS method for detecting metal platinum was established, which can quickly and accurately determine the platinum concentration in samples and provide a fast and reliable detection method for the determination of platinum concentration.

In addition, the occurrence of drug resistance in tumor chemotherapy is also a common phenomenon, and it is an important cause of chemotherapy failure (accounting for 80−90%).[40] The main reason for that is caused by overexpression of multidrug resistance-related proteins (such as MRPs) in gastric cancer cells,[41] which can enhance the resistance of tumor cells to a variety of chemotherapy drugs by reducing the intracellular drug concentration and preventing the drug from binding to the intracellular target.[42] Meanwhile, MRPs were found to be platinum-based transport substrates and involved in platinum-based drug resistance.[9,43,44] Therefore, inhibiting the expression of related proteins is of great significance, and many inhibitors have been developed and applied in the clinic.[45] However, the inhibitors such as cyclosporine A, sorafenib, regorafenib, etc.[46] have obvious toxicity, and the use of single-target inhibitors can easily lead to the development of new drug resistance.[47] The results of this paper suggest that the combination of AKUs and OXA inhibits the expression of efflux proteins MRP1 and MRP2, and the inhibition rate is 48.3 and 27.2%, respectively. Compared with Western medicine, traditional Chinese medicine reversal agents have unique advantages. Traditional Chinese medicine polysaccharides are safe and less harmful to the human body.[48]

In addition, organic cation transporter 2 (OCT2) is the main uptake transporter of platinum anticancer drugs, and inhibition of its expression can lead to a decrease in the uptake of platinum anticancer drugs by cancer cells.[49,50] Therefore, increasing the expression of the molecule of OCT2 may help tumor cells to absorb anticancer drugs. The results showed that the combination of AKUs and OXA could upregulate the expression of OCT2, thereby increasing the uptake of OXA by cancer cells. The results showed that AKUs inhibited the overexpression of drug resistance proteins and the effect of protein intake, suggesting their potential application as a drug resistance inhibitor.

5. CONCLUSIONS

In summary, in this article, by studying the ultrasonic extraction method, the yield of AKUs was improved and the content of effective polysaccharide (such as acidic sugar) was increased. At the same time, it was found that AKUs had a synergistic effect on molecularly targeted drugs and platinum drugs. This synergistic effect was also related to inhibiting the expression of multidrug resistance protein, promoting the expression of uptake protein, and increasing the effective concentration of drugs. These results suggest that AKUs have the potential to be developed as a chemosensitizer.

■ AUTHOR INFORMATION

Corresponding Authors

Ruizhi Zhao − *State Key Laboratory of Dampaness Syndrome of Chinese Medicine, The Second Affiliated Hospital of Guangzhou University of Chinese Medicine, Guangzhou 510006, China;* ● orcid.org/0000-0002-9554-3897;

Phone: +86 2039318571; Email: Zhaoruizhi@gzucm.edu.cn

Yan Wang − *School of Chinese Materia Medica, Guangdong Pharmaceutical University, Guangzhou 510006, China;* Phone: +86 13570587769; Email: Wangyan@gdpu.edu.cn

Authors

Minjie Liang − *School of Chinese Materia Medica, Guangdong Pharmaceutical University, Guangzhou 510006, China;* ● orcid.org/0009-0009-4140-4662

Yayun Wu − *State Key Laboratory of Dampaness Syndrome of Chinese Medicine, The Second Affiliated Hospital of Guangzhou University of Chinese Medicine, Guangzhou 510006, China*

Jimin Sun − *School of Chinese Materia Medica, Guangdong Pharmaceutical University, Guangzhou 510006, China*

Ya Zhao − *State Key Laboratory of Dampaness Syndrome of Chinese Medicine, The Second Affiliated Hospital of Guangzhou University of Chinese Medicine, Guangzhou 510006, China*

Lijuan Liu − *State Key Laboratory of Dampaness Syndrome of Chinese Medicine, The Second Affiliated Hospital of Guangzhou University of Chinese Medicine, Guangzhou 510006, China*

Complete contact information is available at:
https://pubs.acs.org/10.1021/acsomega.4c00364

Author Contributions

§M.L. and Y.W. contributed equally to this work.

Notes

The authors declare no competing financial interest.

■ ACKNOWLEDGMENTS

■ REFERENCES

(1) Yang, W.; Zhao, H.; Yu, Y.; Wang, J.; Guo, L.; Liu, J.; et al. Updates on global epidemiology, risk and prognostic factors of gastric cancer. *World Journal of Gastroenterology* **2023**, *29* (16), 2452−2468.

(2) Qiu, H.; Cao, S.; Xu, R. Cancer incidence, mortality, and burden in China: a time-trend analysis and comparison with the United States and United Kingdom based on the global epidemiological data released in 2020. *Cancer Communications* **2021**, *41* (10), 1037−1048.

(3) Zhang, S. X.; Liu, W.; Ai, B.; Sun, L. L.; Chen, Z. S.; Lin, L. Z. Current Advances and Outlook in Gastric Cancer Chemoresistance: A Review. *Recent patents on anti-cancer drug discovery* **2022**, *17* (1), 26−41.

(4) Xing, P.; Wang, S.; Cao, Y.; Liu, B.; Zheng, F.; Guo, W.; et al. Treatment strategies and drug resistance mechanisms in adenocarcinoma of different organs. *Drug Resist Updat* **2023**, *71*, No. 101002.

(5) Joshi, S. S.; Badgwell, B. D. Current treatment and recent progress in gastric cancer. *CA: A Cancer Journal for Clinicians* **2021**, *71* (3), 264−279.

(6) Ajani, J. A.; D'amico, T. A.; Bentrem, D. J.; Chao, J.; Cooke, D.; Corvera, C.; et al. Gastric Cancer, Version 2.2022. *Journal of the National Comprehensive Cancer Network* **2022**, *20* (2), 167−192.

(7) Lu, J. F.; Pokharel, D.; Bebawy, M. MRP1 and its role in anticancer drug resistance. *Drug metabolism reviews* **2015**, *47* (4), 406−419.

(8) Fan, J.; To, K. K. W.; Chen, Z.-S.; Fu, L. ABC transporters affects tumor immune microenvironment to regulate cancer immunotherapy and multidrug resistance. *Drug Resist. Updates* **2023**, *66*, No. 100905, DOI: 10.1016/j.drup.2022.100905.

(9) Burger, H.; Loos, W. J.; Eechoute, K.; Verweij, J.; Mathijssen, R. H.; Wiemer, E. A. Drug transporters of platinum-based anticancer agents and their clinical significance. *Drug Resist Updat* **2011**, *14* (1), 22−34.

(10) Sui, H.; Zhou, L. H.; Zhang, Y. L.; Huang, J. P.; Liu, X.; Ji, Q.; et al. Evodiamine Suppresses ABCG2Mediated Drug Resistance by Inhibiting p50/p65 NF-κB Pathway in Colorectal Cancer. *Journal of cellular biochemistry* **2016**, *117* (6), 1471−1481.

(11) Zhang, Y.; Li, Q.; Wang, J.; Cheng, F.; Huang, X.; Cheng, Y.; et al. Polysaccharide from Lentinus edodes combined with oxaliplatin possesses the synergy and attenuation effect in hepatocellular carcinoma. *Cancer Lett.* **2016**, *377* (2), 117−125.

(12) Bhatia, K.; Bhumika, D. A; Das, A. Combinatorial drug therapy in cancer - New insights. *Life Sci.* **2020**, *258*, No. 118134.

(13) Su, C.; Liu, S.; Ma, X.; Liu, J.; Liu, J.; Lei, M.; et al. The effect and mechanism of erianin on the reversal of oxaliplatin resistance in human colon cancer cells. *Cell Biol. Int.* **2021**, *45* (12), 2420−2428.

(14) Kang, Y.-K.; Chin, K.; Chung, H. C.; Kadowaki, S.; Oh, S. C.; Nakayama, N.; et al. S-1 plus leucovorin and oxaliplatin versus S-1 plus cisplatin as first-line therapy in patients with advanced gastric cancer (SOLAR): a randomised, open-label, phase 3 trial. *Lancet Oncology* **2020**, *21* (8), 1045−1056.

(15) Sah, B. K.; Xu, W.; Zhang, B.; Zhang, H.; Yuan, F.; Li, J. Feasibility and Safety of Perioperative Chemotherapy With Fluorouracil Plus Leucovorin, Oxaliplatin, and Docetaxel for Locally Advanced Gastric Cancer Patients in China. *Front. Oncol.* **2021**, *10*, No. 567529.

(16) Wei, X.-M.; Jiang, S.; Li, S.-S.; Sun, Y.-S.; Wang, S.-H.; Liu, W.-C.; et al. Endoplasmic Reticulum Stress-Activated PERK-eIF2α-ATF4 Signaling Pathway is Involved in the Ameliorative Effects of Ginseng Polysaccharides against Cisplatin-Induced Nephrotoxicity in Mice. *Acs Omega* **2021**, *6* (13), 8958−8966.

(17) Zhao, Y.; Wan, P.; Wang, J.; Li, P.; Hu, Q.; Zhao, R. Polysaccharide from vinegar baked radix bupleuri as efficient solubilizer for water-insoluble drugs of Chinese medicine. *Carbohydr. Polym.* **2020**, *229*, No. 115473.

(18) Wang, X.; Zhao, Y.; Wu, Y.; Liu, L.; Liang, M.; Han, M. Size, surface charge and flexibility of vinegar-baked Radix Bupleuri polysaccharide affecting the immune response. *Arabian J. Chem.* **2022**, *15* (8), No. 104008, DOI: 10.1016/j.arabjc.2022.104008.

(19) Ahmed, S.; Zhan, C.; Yang, Y.; Wang, X.; Yang, T.; Zhao, Z. The Transcript Profile of a Traditional Chinese Medicine, Atractylodes lancea, Revealing Its Sesquiterpenoid Biosynthesis of the Major Active Components. *PLoS One* **2016**, *11* (3), No. e0151975, DOI: 10.1371/journal.pone.0151975.

(20) Zhang, W.; Zhao, Z.; Chang, L.; Cao, Y.; Wang, S.; Kang, C. Atractylodis Rhizoma: A review of its traditional uses, phytochemistry, pharmacology, toxicology and quality control. *J. Ethnopharmacol.* **2021**, *266*, No. 113415, DOI: 10.1016/j.jep.2020.113415.

(21) Chang, L.; Zhang, W.; Cao, Y.; Wang, S.; Kang, C.; Zhou, L. Extraction and separation, structure analysis and biological activity of polysaccharides from Atractylodis Rhizoma. *Zhongguo Zhong Yao Za Zhi* **2021**, *46* (9), 2133−2141.

(22) Qin, J.; Wang, H.; Zhuang, D.; Meng, F.; Zhang, X.; Huang, H.; et al. Structural characterization and immunoregulatory activity of two polysaccharides from the rhizomes of Atractylodes lancea (Thunb.) DC. *Int. J. Biol. Macromol.* **2019**, *136*, 341−351.

(23) Liu, Y.; Qin, H.; Zhong, Y.; Li, S.; Wang, H.; Wang, H. Neutral polysaccharide from Panaxnotoginseng enhanced cyclophosphamide antitumor efficacy in hepatoma H22-bearing mice. *BMC Cancer* **2021**, *21* (1), 37 DOI: 10.1186/s12885-020-07742-z.

(24) Zhou, P.; Xiao, W.; Wang, X.; Wu, Y.; Zhao, R.; Wang, Y. A Comparison Study on Polysaccharides Extracted from Atractylodes chinensis (DC.) Koidz. Using Different Methods: Structural Characterization and Anti-SGC-7901 Effect of Combination with Apatinib. *Molecules* **2022**, *27* (15), 4727 DOI: 10.3390/molecules27154727.

(25) Wei, Q.; Zhang, Y. H. Ultrasound-assisted polysaccharide extraction from Cercis chinensis and properites, antioxidant activity of polysaccharide. *Ultrason Sonochem* **2023**, *96*, No. 106422.

(26) Wei, N.; Wang, X.; Wu, Y.; Liu, L.; Zhao, Y.; Zhao, R. Comparative Study on Anti-Inflammatory Effect of Polysaccharides from Vinegar-Baked Radix Bupleuri Using Different Methods. *ACS Omega* **2023**, *8* (32), 29253−29261.

(27) Zheng, Q.; Sun, R. Analysis of drug interactions in combined drug therapy by reflection method. *Acta Pharmacol. Sin.* **2000**, *21* (2), 183−187.

(28) Chen, H.; Shi, X.; Zhang, L.; Yao, L.; Cen, L.; Li, L. Ultrasonic Extraction Process of Polysaccharides from Dendrobium nobile Lindl.: Optimization, Physicochemical Properties and Anti-Inflammatory Activity. *Foods* **2022**, *11* (19), 2957 DOI: 10.3390/foods11192957.

(29) Dzah, C.; Duan, Y.; Zhang, H.; Wen, C.; Zhang, J.; Chen, G. The effects of ultrasound assisted extraction on yield, antioxidant, anticancer and antimicrobial activity of polyphenol extracts: A review. *Food Biosci.* **2020**, *35*, No. 100547.

(30) Hu, X.; Xu, F.; Li, J.; Li, J.; Mo, C.; Zhao, M.; et al. Ultrasonic-assisted extraction of polysaccharides from coix seeds: Optimization, purification, and in vitro digestibility. *Food Chem.* **2022**, *374*, No. 131636.

(31) Li, J.; Chen, Z.; Shi, H.; Yu, J.; Huang, G.; Huang, H. Ultrasound-assisted extraction and properties of polysaccharide from Ginkgo biloba leaves. *Ultrason Sonochem* **2023**, *93*, No. 106295.

(32) Wu, F.; Zhou, C.; Zhou, D.; Ou, S.; Zhang, X.; Huang, H. Structure characterization of a novel polysaccharide from Hericium erinaceus fruiting bodies and its immunomodulatory activities. *Food & Function* **2018**, *9* (1), 294−306.

(33) Yang, X.; Huang, M.; Qin, C.; Lv, B.; Mao, Q.; Liu, Z. Structural characterization and evaluation of the antioxidant activities of polysaccharides extracted from Qingzhuan brick tea. *Int. J. Biol. Macromol.* **2017**, *101*, 768−775.

(34) Jetter, A.; Kullak-Ublick, G. A. Drugs and hepatic transporters: A review. *Pharmacol. Res.* **2020**, *154*, 104234 DOI: 10.1016/j.phrs.2019.04.018.

(35) Morrissey, K.; Stocker, S.; Wittwer, M.; Xu, L.; Giacomini, K. Renal Transporters in Drug Development. *Annual Review of Pharmacology and Toxicology* **2013**, *53* (1), 503.

(36) Wang, Z.; Zhou, X.; Sheng, L.; Zhang, D.; Zheng, X.; Pan, Y. Effect of ultrasonic degradation on the structural feature, physicochemical property and bioactivity of plant and microbial polysaccharides: A review. *Int. J. Biol. Macromol.* **2023**, *236*, No. 123924, DOI: 10.1016/j.ijbiomac.2023.123924.

(37) Yue, F.; Xu, J.; Zhang, S.; Hu, X.; Wang, X.; Lue, X. Structural features and anticancer mechanisms of pectic polysaccharides: A review. *Int. J. Biol. Macromol.* **2022**, *209*, 825−839.

(38) Li, J.; Qin, S.; Xu, J.; Xiong, J.; Wu, C.; Bai, Y.; et al. Randomized, Double-Blind, Placebo-Controlled Phase III Trial of Apatinib in Patients With Chemotherapy-Refractory Advanced or Metastatic Adenocarcinoma of the Stomach or Gastroesophageal Junction. *Journal of Clinical Oncology* **2016**, *34* (13), 1448.

(39) Xiao, Y.; Li, B.; Liu, J.; Wang, S.; Liu, J.; Yang, H. Role of lncSLCO1C1 in gastric cancer progression and resistance to oxaliplatin therapy. *Clin. Transl. Med.* **2022**, *12* (4), No. e691, DOI: 10.1002/ctm2.691.

(40) Zhou, F.; Teng, F.; Deng, P.; Meng, N.; Song, Z.; Feng, R. Recent Progress of Nano-drug Delivery System for Liver Cancer Treatment. *Anti-Cancer Agents Med. Chem.* **2017**, *17* (14), 1884−1897.

(41) Wu, C.; Hsiao, S.; Wu, Y. Perspectives on drug repurposing to overcome cancer multidrug resistance mediated by ABCB1 and ABCG2. *Drug Resist Updat* **2023**, *71*, No. 101011.

(42) Li, W.; Zhang, H.; Assaraf, Y. G.; et al. Overcoming ABC transporter-mediated multidrug resistance: Molecular mechanisms and novel therapeutic drug strategies. *Drug Resistance Updates* **2016**, *27*, 14−29.

(43) Wang, M.; Xiang, Y.; Wang, R.; Zhang, L.; Zhang, H.; Chen, H.; et al. Dihydrotanshinone I Inhibits the Proliferation and Growth of Oxaliplatin-Resistant Human HCT116 Colorectal Cancer Cells. *Molecules* **2022**, *27* (22), 7774 DOI: 10.3390/molecules27227774.

(44) Shimizu, T.; Fujii, T.; Sakai, H. The Relationship Between Actin Cytoskeleton and Membrane Transporters in Cisplatin Resistance of Cancer Cells. *Frontiers in cell and developmental biology* **2020**, *8*, No. 597835.

(45) Huang, W.; Ruan, S.; Wen, F.; Lu, X.; Gu, S.; Chen, X.; et al. Multidrug Resistance of Gastric Cancer: The Mechanisms and Chinese Medicine Reversal Agents. *Cancer Management and Research* **2020**, *12*, 12385−12394.

(46) Miners, J. O.; Chau, N.; Rowland, A.; Burns, K.; Mckinnon, R. A.; Mackenzie, P. I.; et al. Inhibition of human UDP-glucuronosyl-transferase enzymes by lapatinib, pazopanib, regorafenib and sorafenib: Implications for hyperbilirubinemia. *Biochem. Pharmacol.* **2017**, *129*, 85−95.

(47) Zhang, H.; Xu, H.; Ashby, C. R., Jr.; Assaraf, Y. G.; Chen, Z.-S.; Liu, H.-M. Chemical molecular-based approach to overcome multidrug resistance in cancer by targeting P-glycoprotein (P-gp). *Medicinal Research Reviews* **2021**, *41* (1), 525−555.

(48) Bharathiraja, P.; Yadav, P.; Sajid, A.; Ambudkar, S. V.; Prasad, N. R. Natural medicinal compounds target signal transduction pathways to overcome ABC drug efflux transporter-mediated multidrug resistance in cancer. *Drug Resist Updat* **2023**, *71*, No. 101004.

(49) Yonezawa, A.; Masuda, S.; Yokoo, S.; Katsura, T.; Inui, K-i Cisplatin and oxaliplatin, but not carboplatin and nedaplatin, are substrates for human organic cation transporters (SLC22A1−3 and multidrug and toxin extrusion family). *Journal of Pharmacology and Experimental Therapeutics* **2006**, *319* (2), 879−886.

(50) Martinez-balibrea, E.; Martínez-cardús, A.; Ginés, A.; Ruiz de porras, V.; Moutinho, C.; Layos, L.; et al. Tumor-Related Molecular Mechanisms of Oxaliplatin Resistance. *Mol. Cancer Ther* **2015**, *14* (8), 1767−1776.